

MEASUREMENT OF THE  $\omega^0$  AND  $\eta^0$  BRANCHING RATIOS AND

A STUDY OF THE REACTION  $K^- + p \rightarrow \bar{K}^0 + n$

B. Buschbeck-Czapp and I. Wacek (University of Vienna)

W.A. Cooper, A. Fridman<sup>+</sup>, E. Malamud<sup>\*</sup> and G. Otter (CERN)

E. Gelsema and A. Tenner (University of Amsterdam)

+ On leave of absence from the Centre de Recherches Nucléaires, Strasbourg

\* On leave of absence from the Université de Lausanne and  
FORD Foundation Fellow

1

2

3

- 1 -

## I. Introduction

We have studied the interactions of 1.455 GeV/c  $K^-$  mesons with protons in the CERN 30 cm hydrogen bubble chamber. The beam has been described previously <sup>(1)</sup>. The events have been processed by the CERN THRESH-GRIND system followed by the system of library programs CULL-CSORT-UPDATE-SUMX.

## II. The $\omega^0$ and $\eta^0$ branching ratios

Among the interactions giving a  $\Lambda^0$  together with two charged particles 709 fit the hypothesis  $K^- p \rightarrow \Lambda^0 \pi^+ \pi^- \pi^0$ . The effective mass plot in Fig. 1 shows that 51 o/o of these pass via the reaction  $K^- + p \rightarrow \Lambda^0 + \omega$ . A small number of events fall in the region of the  $\eta$  mass. The Dalitz plot of the  $\omega$  decay shows the well established decrease in population towards the boundary. The  $\eta$  plot shows a concentration of events towards low  $\pi^0$  KE as has also been found by other workers <sup>(2)</sup>.

465 zero prong events with associated  $\Lambda^0$  have been found and Fig. 2 shows the missing mass plot for these events. The peaks at the  $\omega^0$  and  $\eta^0$  masses are clearly visible. These correspond, of course, to decays into neutral particles. The direct way to determine the branching ratio, as has been used by other authors <sup>(3,4)</sup>, is to compare these two plots. This is liable to lead to systematic errors since the resolution in the effective mass is necessarily better than in the missing mass, and because the zero prong events, which need only a decay fit are more likely to pass the kinematics programmes than the two prong events where a decay and interaction fit are required. We therefore treated both 0-prong and 2-prong events in the same way by demanding only a  $\Lambda^0$  decay fit and plotting their c.m.s. KE (which is equivalent to the missing mass in this case). This was done by modifying the CULL program to choose best decay fits automatically. Experience has shown this to be reliable. These two plots are shown in Fig. 3. Zero prong events were measured in less pictures than two prong events. The ratio of the beam tracks in the two groups of pictures is  $1.40 \pm .05$  and the results must be multiplied by this factor.

$\Lambda^0$  with very low or very high momenta are more difficult to fit than others, and those which have very low energy pi mesons have reduced scanning efficiency.

- 2 -

These effects depend on the laboratory kinetic energy and so are identical in the two cases (0-prong and 2-prong).

Since the kinematics of the  $\Lambda^0 + \omega (\eta)$  is the same whether it is produced in a 2-prong or 0-prong event, the biases are the same and no correction is necessary to the ratio.

Using this method the 2-prong events give the combined  $\pi^+ \pi^- \pi^0$  and  $\pi^+ \pi^- \gamma$  decay modes. The results are given in Table I.

Table I

	$\eta$	$\omega$
0-prong	37	20
2-prong	20	254
Corrected ratio $\frac{\eta \rightarrow \text{neutrals}}{\pi^+ \pi^- \pi^0 + \pi^+ \pi^- \gamma}$	$2.6 \pm 0.9$	$0.11 \pm .02$

We compare our results with other experiments (summarised in ref. (5)).

To find the ratio  $\frac{\eta \rightarrow \text{neutrals}}{\eta \rightarrow \pi^+ \pi^- \pi^0}$  we correct our ratio using the measured value

$$\frac{\eta \rightarrow \pi^+ \pi^- \gamma}{\eta \rightarrow \pi^+ \pi^- \pi^0} = 0.26 \text{ and the result becomes } \frac{\eta \rightarrow \text{neutrals}}{\eta \rightarrow \pi^+ \pi^- \pi^0} = 3.3 \text{ which is slightly}$$

higher than found by other groups.

Our experimental results are insufficient to see the mode  $\omega \rightarrow \pi^+ \pi^-$  in the events of the type  $K^- p \rightarrow \Lambda^0 \pi^+ \pi^-$  but we can give an upper limit

$$\omega \rightarrow \pi^+ \pi^- < 0.09 \omega \rightarrow \pi^+ \pi^- \pi^0.$$

#### $K^-$ charge exchange process

Among the zero prong events with associated  $V^0$ , 367 are found to be  $K^- + p \rightarrow \bar{K}^0 + \text{neutrals}$ . Fig. 4 shows the distribution of neutral mass and a well defined peak at the neutron mass is seen. It is therefore possible to make a clean  
PS/4030/sm

separation of the charge exchange reactions  $\bar{K} + p \rightarrow \bar{K}^0 + n$ . There are in fact 161 events with  $0.75 < MM^2 < 1.1 \text{ GeV}^2$ . The charge exchange cross section is  $1.95 \pm 0.20 \text{ mb}$ . Fig. 5 shows the production angular distribution.

Fig. 6 is a scatter diagram of events on a  $P_t - P_L^*$  plot. The events in the charge exchange peak are shown as dots and fall clearly on a semicircle defined by the kinematics. Events outside the circle must be wrong identifications. The uniform distribution of inelastic events (represented by crosses) inside the circle implies that high angular momentum states are not important in the inelastic processes.

#### Acknowledgements

It is a pleasure to acknowledge valuable discussions with Dr. R. Armenteros and Prof. H. Filthuth.

References

- (1) G. Amato et al.  
Nuclear Instruments and Meth. 20, 47 (1963)
- (2) D.B. Lichtenberg - SLAC 13 (1963)
- (3) C. D'Andlauer, A. Astier, C. Ghesquière, B. Gregory, D. Rahm, B. Rivet,  
F. Solmitz, R. Armenteros, R. Budde, L. Montanet, D. Morrison, S. Nilsson,  
A. Shapira and J. Vandermeulen  
Comptes Rendus Académie des Sciences t. 256 p. 1279 (see also this conference)
- (4) J. Murray et al. - UCRL 10723 (1963)
- (5) M. Roos - Rev. of Modern Physics 35, 314 (1963)
- (6) M.L. Goldberger - Ecole d'été de physique théorique Les Houches:  
Relations de dispersion et particules élémentaires, p.140
- (7) E. Fowler, F. Crawford, L. Lloyd, R. Grossman, L. Price  
Phys. Rev. Letters 10, 110 (1963)

Figure Captions

- Fig. 1 The effective mass distribution for the  $3\pi$  combination in 709 events  $\bar{K}p \rightarrow \Lambda^0 \pi^+ \pi^- \pi^0$  (2-prong +  $V^0$ ).
- Fig. 2 The (missing mass)<sup>2</sup> distribution in the reaction  $\bar{K}p \rightarrow \Lambda^0 + \text{neutrals}$  (0-prong +  $V^0$ ).
- Fig. 3 The  $\Lambda^0$  kinetic energy distribution in the reactions  $\bar{K}p \rightarrow \Lambda^0 + 2 \text{ charged tracks (+ neutrals)}$  and  $\bar{K}p \rightarrow \Lambda^0 + \text{neutrals}$ .
- Fig. 4 The (missing mass)<sup>2</sup> distribution in the reaction  $\bar{K}p \rightarrow \bar{K}^0 + \text{neutrals}$  (0-prong +  $V^0$ ).
- Fig. 5 The center of mass production angular distribution for the reaction  $\bar{K}p \rightarrow \bar{K}^0 n$ . Events are defined as those in the elastic peak in Fig. 4.
- Fig. 6  $P_{\perp} - P_L$  plot of all events  $\bar{K}p \rightarrow \bar{K}^0 + \text{neutrals}$ . Events defined as  $\bar{K}^0 n$  are shown as dots, other events as crosses.

The first part of the document discusses the importance of maintaining accurate records of all transactions. It emphasizes that every entry should be supported by a valid receipt or invoice. This ensures transparency and allows for easy verification of the data.

In the second section, the author details the various methods used to collect and analyze the data. This includes both manual and automated processes. The goal is to ensure that the data is as accurate and reliable as possible.

The third part of the document focuses on the results of the analysis. It shows that there is a clear trend in the data, which is consistent with the initial hypothesis. This finding is significant as it provides strong evidence for the proposed model.

Finally, the document concludes with a summary of the findings and a list of recommendations for future research. It suggests that further studies should be conducted to explore the underlying causes of the observed trends.



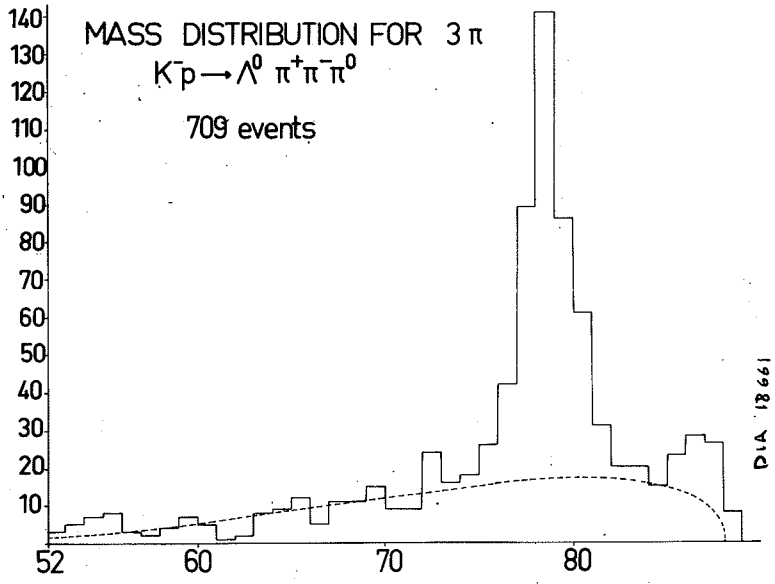


Fig.1

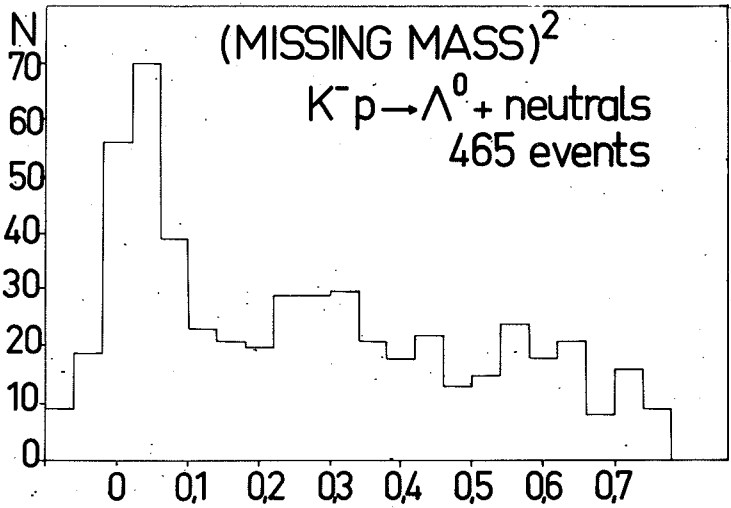


Fig.2

1971  
1972  
1973

1974  
1975  
1976

1977  
1978  
1979  
1980  
1981  
1982  
1983  
1984  
1985  
1986  
1987  
1988  
1989  
1990  
1991  
1992  
1993  
1994  
1995  
1996  
1997  
1998  
1999  
2000  
2001  
2002  
2003  
2004  
2005  
2006  
2007  
2008  
2009  
2010  
2011  
2012  
2013  
2014  
2015  
2016  
2017  
2018  
2019  
2020  
2021  
2022  
2023  
2024  
2025  
2026  
2027  
2028  
2029  
2030  
2031  
2032  
2033  
2034  
2035  
2036  
2037  
2038  
2039  
2040  
2041  
2042  
2043  
2044  
2045  
2046  
2047  
2048  
2049  
2050

1971  
1972  
1973  
1974  
1975  
1976  
1977  
1978  
1979  
1980  
1981  
1982  
1983  
1984  
1985  
1986  
1987  
1988  
1989  
1990  
1991  
1992  
1993  
1994  
1995  
1996  
1997  
1998  
1999  
2000  
2001  
2002  
2003  
2004  
2005  
2006  
2007  
2008  
2009  
2010  
2011  
2012  
2013  
2014  
2015  
2016  
2017  
2018  
2019  
2020  
2021  
2022  
2023  
2024  
2025  
2026  
2027  
2028  
2029  
2030  
2031  
2032  
2033  
2034  
2035  
2036  
2037  
2038  
2039  
2040  
2041  
2042  
2043  
2044  
2045  
2046  
2047  
2048  
2049  
2050

1971  
1972  
1973

1974  
1975  
1976  
1977  
1978  
1979  
1980  
1981  
1982  
1983  
1984  
1985  
1986  
1987  
1988  
1989  
1990  
1991  
1992  
1993  
1994  
1995  
1996  
1997  
1998  
1999  
2000  
2001  
2002  
2003  
2004  
2005  
2006  
2007  
2008  
2009  
2010  
2011  
2012  
2013  
2014  
2015  
2016  
2017  
2018  
2019  
2020  
2021  
2022  
2023  
2024  
2025  
2026  
2027  
2028  
2029  
2030  
2031  
2032  
2033  
2034  
2035  
2036  
2037  
2038  
2039  
2040  
2041  
2042  
2043  
2044  
2045  
2046  
2047  
2048  
2049  
2050

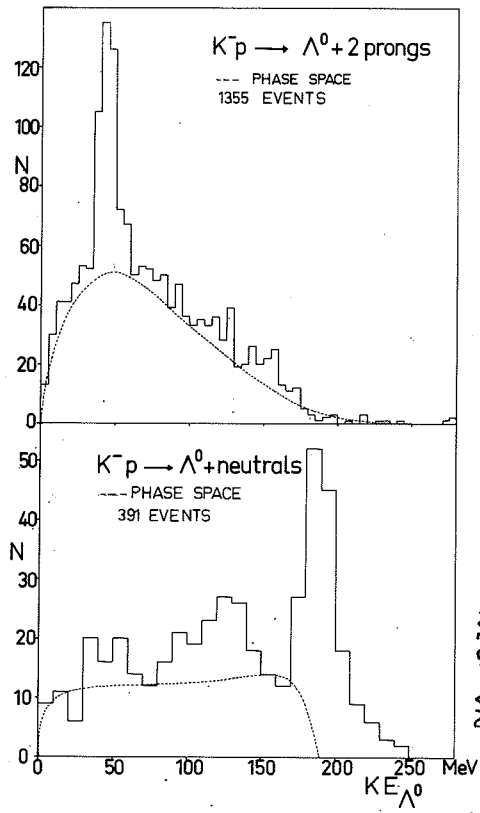


Fig.3

4  
A  
E  
T

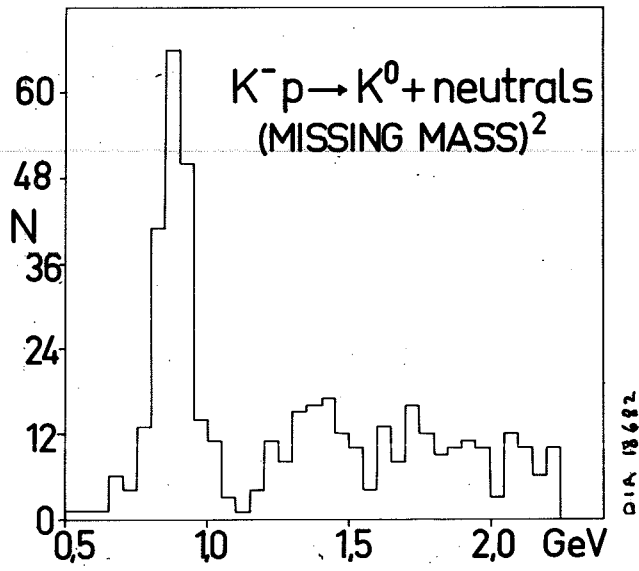


Fig.4

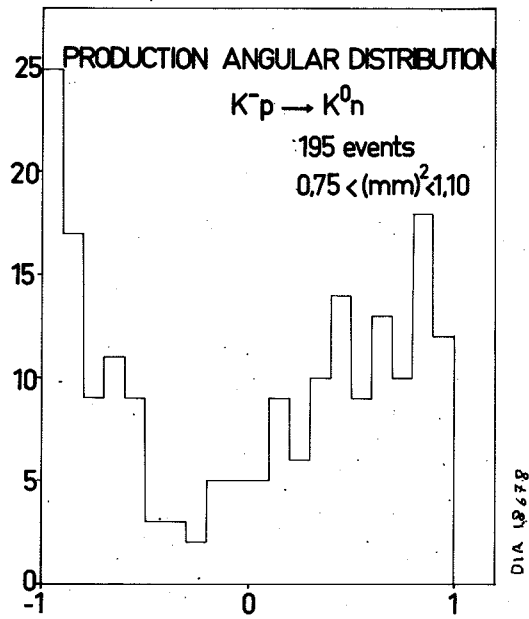


Fig.5

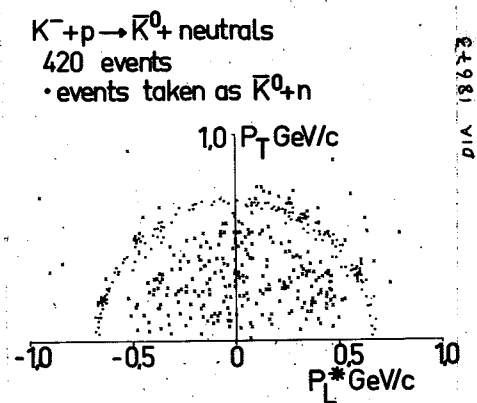


Fig.6

108

Fig 1

109  
110  
111  
112  
113  
114  
115  
116  
117  
118  
119  
120

Fig 2

121  
122  
123  
124  
125  
126  
127  
128  
129  
130  
131  
132  
133  
134  
135  
136  
137  
138  
139  
140  
141  
142  
143  
144  
145  
146  
147  
148  
149  
150  
151  
152  
153  
154  
155  
156  
157  
158  
159  
160  
161  
162  
163  
164  
165  
166  
167  
168  
169  
170  
171  
172  
173  
174  
175  
176  
177  
178  
179  
180  
181  
182  
183  
184  
185  
186  
187  
188  
189  
190  
191  
192  
193  
194  
195  
196  
197  
198  
199  
200

Fig 3

201  
202  
203  
204  
205  
206  
207  
208  
209  
210  
211  
212  
213  
214  
215  
216  
217  
218  
219  
220  
221  
222  
223  
224  
225  
226  
227  
228  
229  
230  
231  
232  
233  
234  
235  
236  
237  
238  
239  
240  
241  
242  
243  
244  
245  
246  
247  
248  
249  
250  
251  
252  
253  
254  
255  
256  
257  
258  
259  
260  
261  
262  
263  
264  
265  
266  
267  
268  
269  
270  
271  
272  
273  
274  
275  
276  
277  
278  
279  
280  
281  
282  
283  
284  
285  
286  
287  
288  
289  
290  
291  
292  
293  
294  
295  
296  
297  
298  
299  
300

108  
109  
110  
111  
112  
113  
114  
115  
116  
117  
118  
119  
120

